ENGINEER - Vol. LVIII, No. 04, pp. [69-79], 2025

DOI: https://doi.org/10.4038/engineer.v58i4.7718

Evaluation of NASA POWER Reanalysis Data for Daily Weather Variables and Observed Long-Term Climate Trends in Nuwara Eliya, Sri Lanka

D.K.A.I. Ravindu and D.D. Dias

Abstract: Accurate climate data is essential for planning climate resilience and understanding regional climate variability, particularly in high-altitude, data-scarce regions such as Nuwara Eliya, Sri Lanka. This study evaluates the performance of NASA POWER reanalysis data (0.5° latitude × 0.625° longitude resolution) by comparing it with ground-based meteorological observations from 2009 to 2021, addressing a gap that remains largely unexplored in the existing literature. Key climate variables, including precipitation, temperature, wind speed, and relative humidity (daily data), along with cloud cover (monthly data, 2017–2020), were validated using the correlation coefficient (R), mean error (ME), root mean square error (RMSE), and percent bias (PBIAS). The results showed strong agreement for temperature (bias-corrected $R = 0.66$), wind speed ($R = 0.72$), cloud cover ($R = 0.92$), and relative humidity ($R = 0.63$). Precipitation analysis revealed that dry-day overestimation drove positive biases in FIM, SIM, and NEM, whereas SWM biases resulted from underestimation of monsoon rainfall intensity. The Mann-Kendall test and Sen's slope estimator were applied to detect long-term trends (1990–2020), revealing a significant increase in minimum temperature (0.01 °C/year) and shortwave radiation (0.2 W/m²/year), and a decline in wind speed (−0.03 m/s/year), indicating significant climate shifts in the region. This study provides a comprehensive validation of NASA POWER data in Sri Lanka's central highlands, underscores the need for localised bias correction, and demonstrates its potential for broader application in similar high-elevation, data-constrained regions for climate impact assessment and resource planning.

Keywords: Climate change, Mann-Kendall test, Meteorological data validation, Sen's slope

1. Introduction

Climate change and its associated impacts on meteorological variables have become a cynosure area of research, particularly as the frequency and intensity of extreme weather events continue to rise under anthropogenic influences [1]. Understanding these changes is pivotal for mitigating risks to vulnerable sectors such as agriculture, water resources, and human health. Reliable meteorological data is fundamental to this understanding [1], yet many regions face challenges due to a lack of observational data or poor data quality [2]. Reanalysis combines observations with advanced models to produce consistent, long-term climate datasets. These products enhance data quality and homogeneity, but may still require corrections using observational data to address anomalies from land surface modelling [2]. In this context, reanalysis datasets have emerged as invaluable tools for providing consistent and comprehensive meteorological information.

There are several historical reanalysis datasets available, including the Climate Forecast System Reanalysis (CFSR), ERA-Interim products from the European Centre for Medium-Range Weather Forecasts (ECMWF), the Japanese Meteorological Agency's JRA-55, NCEP/NCAR reanalysis, NASA's Modern Era Retrospective-Analysis for Research and Applications (MERRA), and the NASA Prediction of Worldwide Energy Resource (NASA POWER). NASA POWER, accessible at 0.5° latitude by 0.625° longitude through its website, provides daily near-surface data on air temperature, relative humidity, rainfall, solar radiation, wind speed, and cloud cover [2].

Among the various reanalysis datasets available, the NASA Prediction of Worldwide Energy Resource (NASA POWER) stands out due to its

Eng. D.K.A.I. Ravindu, AMIE(SL), B.Sc. Eng. (Ruhuna), M.Sc. Eng. (Peradeniya), Postgraduate Student, Faculty of Engineering, University of Peradeniya.
Email:dkaishanravindu@eng.pdn.ac.lk
https://orcid.org/0009-0000-7084-1639
Mr. D.D. Dias, B.Sc. Eng. (Hons) (Peradeniya), M.Eng.(Hokkaido), Lecturer, Department of Civil Engineering, University of Peradeniya.
Email:daham@pdn.ac.lk
https://orcid.org/0000-0002-6339-3513

accessibility, user-friendly interface, and comprehensive coverage of daily meteorological variables such as air temperature, relative humidity, rainfall, solar radiation, wind speed, and cloud cover [2]. Derived from numerical weather prediction models and a compilation of meteorological observations, NASA POWER offers a reliable representation of global and regional weather conditions, making it a valuable resource for researchers and practitioners in fields ranging from environmental modelling to agricultural planning [2].

Despite its advantages, the accuracy of reanalysis datasets such as NASA POWER can vary across regions and meteorological variables. Several studies have evaluated NASA POWER in different geographical contexts. For example, research in Southern Portugal demonstrated good agreement with ground observations but found that bias correction methods further improved accuracy, particularly for agricultural and environmental applications [2]. Similarly, studies in the USA, China, and Italy reported strong correlations between NASA POWER and observed values for temperature and solar radiation, while discrepancies were more evident for relative humidity, especially in coastal areas [3–5]. These findings highlight the potential of reanalysis data for climate and environmental studies, but they also emphasise the need for region-specific validation and correction. However, in Sri Lanka, and particularly in the complex highland region of Nuwara Eliya, the applicability of NASA POWER remains largely underexplored.

Sri Lanka is highly vulnerable to climate variability and change, with significant implications for agriculture, water resources, and livelihoods. Previous studies [1] have documented increasing trends in air temperature, especially minimum temperature, across different parts of the country. Rainfall patterns, however, remain inconsistent, with some regions experiencing declining long-term trends and others showing increases in heavy rainfall events. Understanding these changes is essential for water resource planning, ecosystem management, and sustaining agricultural productivity in the central highlands, where Nuwara Eliya plays a vital role as a headwater region and as Sri Lanka’s primary tea-producing district.

The primary aim of this study is to evaluate the applicability of NASA POWER reanalysis data in a data-scarce region of Sri Lanka, with a focus on Nuwara Eliya. To achieve this aim, the study validates NASA POWER daily weather variables—air temperature, rainfall, relative humidity, and wind speed—along with monthly cloud cover against ground-based meteorological observations. It further examines long-term climate trends in Nuwara Eliya using observed station data, providing insights into local climate variability. By integrating these two components, the study not only assesses the reliability of NASA POWER data in complex tropical highland regions but also contributes to a better understanding of long-term climate trends in Nuwara Eliya.

2. Materials and Methods

2.1 Study Area

Nuwara Eliya, located in the Central Province of Sri Lanka at an altitude of 1,800 metres (as shown in Figure 1), experiences a cooler climate compared to the lowlands of the country, with a mean annual temperature of 15°C. The region's temperature variations are primarily influenced by altitude, with a mean daily temperature range of 10°C. Ground frost occurs occasionally during the early mornings or nights from January to March, further highlighting the region's unique climatic conditions [6].

2.2 Observed Climatic Data

Daily precipitation, average air temperature, average wind speed, and average relative humidity data for the Nuwara Eliya weather station (WS) were obtained from the Department of Meteorology, Sri Lanka, covering the period January 2009 to December 2021. Additionally, monthly cloud cover data for the same station were collected for the period from 2017 to 2020. These observed datasets were used as the reference to evaluate the accuracy and reliability of NASA POWER reanalysis data.

Furthermore, monthly meteorological data, including average monthly maximum temperature, minimum temperature, rainfall, wind speed, and relative humidity, were summoned from the Natural Resource Management Centre, Department of Agriculture, at the Seetha Eliya WS for the period from 1990 to 2020. This dataset was utilised to analyse long-term trends in meteorological variables by applying statistical

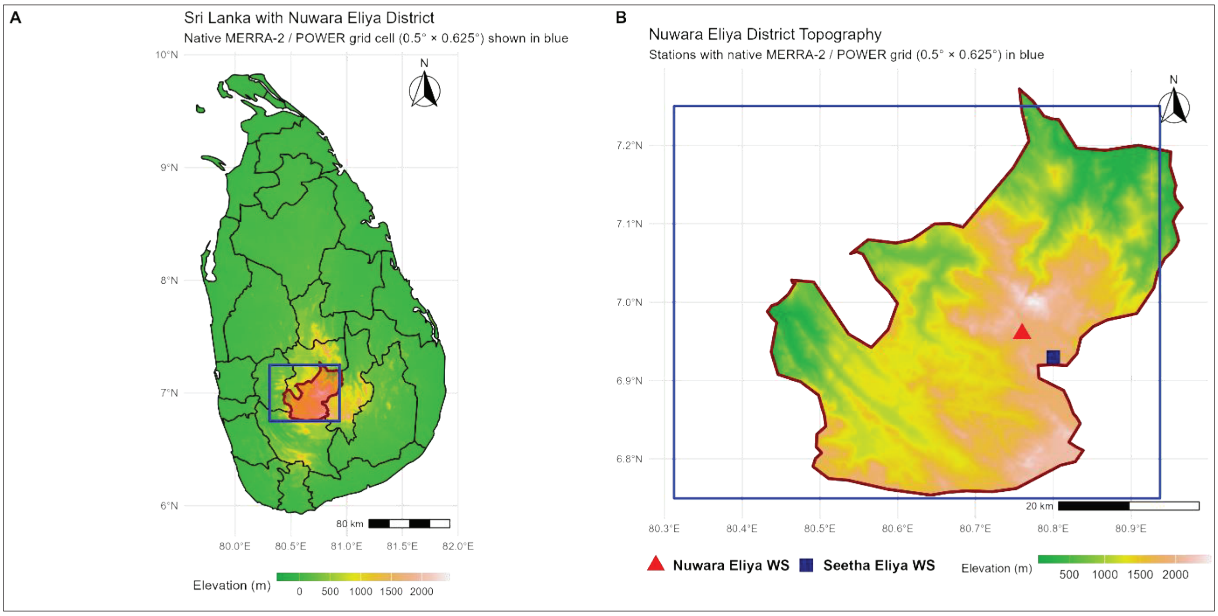

Figure 1 - Geographical Setting of the Study: (A) Sri Lanka with Nuwara Eliya District Highlighted and The Native NASA POWER/MERRA-2 Grid Cell; (B) Topography of Nuwara Eliya District Showing Weather Stations and Grid Coverage

trend detection methods, including the Mann–Kendall test to identify monotonic trends and the Sen's slope estimator to quantify their magnitude.

2.3 Data Cleaning Process

The observed precipitation data were carefully screened to ensure consistency with NASA POWER reanalysis records. Since the analysis was performed daily. Missing days in the observed records—caused by equipment issues, maintenance, or other operational gaps—were excluded, and the corresponding days were also removed from the reanalysis dataset, preserving only matched daily pairs for analysis. To ensure that the resulting statistics remained representative, only months with at least 25 valid precipitation days were retained, following the guidelines of the Natural Resources Conservation Service National Water and Climate Centre, USDA [7]. For temperature, wind speed, and relative humidity, a threshold of at least 21 valid days per month was applied, with daily comparisons again restricted to matched observed–reanalysis pairs. While data-gap filling methods such as nearest-station patching are sometimes recommended, they were not used here due to the unique high-elevation conditions of Nuwara Eliya. Omitting incomplete days ensured that the validation relied solely on actual observations, avoiding the introduction of artificial variability or bias.

2.4 Validation Metrics

The following statistical indicators were used for evaluation.

- Correlation Coefficient (R): Measures the linear correlation between satellite-based climatic variables and gauge observations.

$$R = \frac{\sum(X_i - \bar{X})(Y_i - \bar{Y})}{\sqrt{\sum(X_i - \bar{X})^2 \sum(Y_i - \bar{Y})^2}} \quad \ldots (1)$$

where X_i and Y_i are the individual sample points of observed and predicted values, and $\bar{X}$ and $\bar{Y}$ are their respective means [8].

- Mean Error (ME): Indicates the average difference between observed and predicted values.

$$\text{ME} = \frac{1}{n}\sum_{i=1}^{n} |y_i - \hat{y}_i| \quad \ldots (2)$$

where n is the number of observations, y_i is the observed value, and $\hat{y}_i$ is the predicted value [8].

- Root Mean Square Error (RMSE): Measures the average error magnitude.

$$\mathrm{RMSE} = \sqrt{\frac{1}{n}\sum_{i=1}^{n}(y_i - \hat{y_l})^2} \qquad \dots (3)$$

where n is the number of observations, y_i is the observed value, and $\hat{y_l}$ is the predicted value [8].

Percent Bias (PBIAS): Evaluates the systematic bias of satellite estimates.

$$\mathrm{PBIAS} = 100 \times \frac{\sum_{i=1}^{n}(y_i - \hat{y_l})}{\sum_{i=1}^{n} y_i} \qquad \dots (4)$$

where y_i is the observed value, and $\hat{y_l}$ is the predicted value [8].

2.5 Bias-Correction (Delta Method)

The delta method was used to bias-correct the NASA POWER temperature values using Eq. (5):

$$x_{y,m,d}^{bc} = x_{y,m,d}^{nasa} + \mu_m^{obs} - \mu_m^{nasa} \qquad \dots (5)$$

where the subscripts y, m, and d are the year, month, and day, respectively. x^{bc} is the bias-corrected value. x^{nasa} is the reanalysis value, and μ_m^{obs} and μ_m^{nasa} are the observed and reanalysis monthly average temperature values, respectively [9].

2.6 Mann-Kendall Test

The Mann–Kendall (MK) test was employed to analyse long-term trends in key meteorological variables, including maximum temperature, minimum temperature, precipitation, wind speed, relative humidity, and shortwave radiation, at the Seetha Eliya WS. The MK test is a non-parametric statistical method used to identify trends in time series data without assuming a specific trend shape [10].

The MK statistic S was calculated using Eq. (6):

$$\mathrm{S} = \sum_{j=1}^{N}\sum_{k=j+1}^{N} sgn(y_j - y_k) \qquad \dots (6)$$

where N is the number of points, and y_j and y_k are sequential data values. Let $\varphi = y_j - y_k$. The sign function is defined as:

$$Sgn(\varphi)\begin{cases} 1 \; if \; \varphi > 0 \\ 0 \; if \; \varphi = 0 \\ -1 \; if \; \varphi < 0 \end{cases} \qquad \dots (7)$$

The variance of S, Var(S) was calculated using Eq. (8):

$$\mathrm{Var(S)} = \frac{N(N-1)(2N+5) - \sum_{k=1}^{n} t_k(t_k - 1)(2t_k + 5)}{18} \quad (8)$$

N is the total number of data points, n is the number of tied groups, t_k is the number of data points in the k-th tied group.

The standardised test statistic Z was computed using Eq. (9):

$$\mathrm{Z} = \begin{cases} \frac{(S-1)}{\sqrt{Var(S)}} & if \; S > 0 \\ 0 & if \; S = 0 \\ \frac{(S+1)}{\sqrt{Var(S)}} & if \; S < 0 \end{cases} \qquad \dots (9)$$

The Z statistic is used to assess the significance of the trend at a chosen confidence level (e.g., a 95% confidence level corresponds to a critical Z value of 1.645) [10].

2.7 Sen's Slope Estimator

Sen's nonparametric method was used to estimate the magnitude and direction of trends in the time series data. The slope estimate (Q) was calculated by computing the slopes of all possible pairs of data values:

$$Q_{\mathrm{i}} = \frac{y_j - y_i}{t_j - t_i} \qquad \dots (10)$$

where y_j and y_i are data values at times t_j and t_i, respectively. The median of Q_{i} represents Sen's slope estimate [10].

3. Results and Discussion

3.1 Evaluation of Precipitation

The NASA POWER reanalysis data showed a consistent tendency to overestimate precipitation on dry days, with the extent of the bias varying across months (Figure 2). The highest overestimation was found in November, where the median NASA precipitation reached 3.12 mm/day with a high standard deviation of 6.69 mm/day, indicating a widespread and substantial variability in the false rainfall estimates. Other months with notable overestimation included April (median = 2.12 mm/day, SD = 5.06 mm/day) and October (median = 1.30 mm/day, SD = 3.99 mm/day).

In contrast, the lowest overestimation occurred in January, with a median of only 0.03 mm/day, although the variability was still moderate (SD = 2.76 mm/day). The lowest variability overall was observed in July, where the standard deviation dropped to 1.88 mm/day, suggesting that NASA POWER produced relatively stable (though still spurious) precipitation values during this month.

The comparison of daily precipitation values on wet days (Figure 2) revealed that NASA POWER reanalysis data generally overestimated precipitation, although the magnitude of bias varied considerably between months. The largest overestimation was observed in October and November, where median NASA precipitation values reached 9.92 mm/day and 10.99 mm/day, respectively, compared to observed medians of 6.10 mm/day in both months. These months also exhibited high variability, with standard deviations exceeding 9 mm/day, indicating a wide spread of daily differences. Similarly, December and January exhibited systematic overestimation, with median NASA values approximately 2–4 mm/day higher than the observed values.

In contrast, the smallest differences occurred during the southwest monsoon months (June–August), where median observed precipitation values were 2.79–3.30 mm/day, while NASA estimates were slightly higher at 2.70–3.72 mm/day. Standard deviations in this period were lower (≈4–5 mm/day for NASA), suggesting relatively consistent performance. The lowest variability overall was observed in August (NASA SD = 4.81 mm/day), indicating closer agreement between observed and NASA data.

Table 1 highlights monthly variations in the performance of NASA POWER precipitation estimates. During the First Inter-Monsoon (FIM) season, March and April exhibited moderate to weak correlations of 0.39 and 0.24, respectively, alongside substantial overestimations, with PBIAS values of 45.47% and 61.71%, indicating large positive biases despite low agreement with observations.

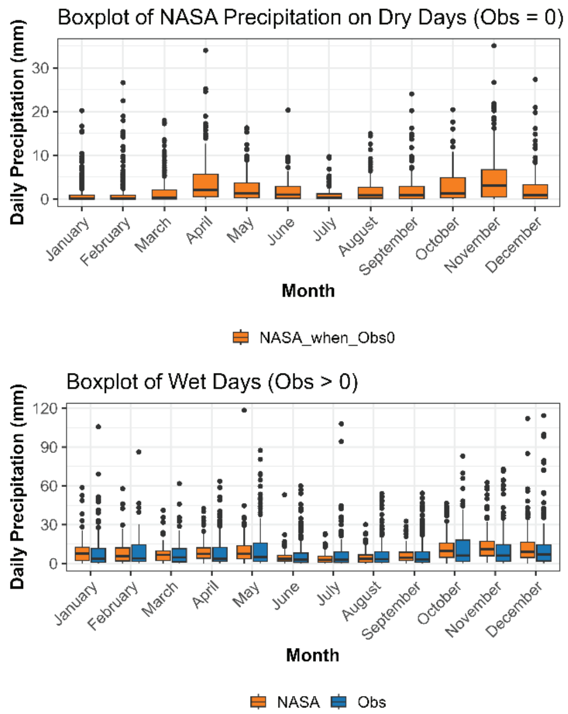

Figure 2 - Boxplots of Daily Precipitation: NASA Power Bias (Dry Days) and Observed vs. NASA Power (Wet Days) (2009-2021)

In the Southwest Monsoon (SWM) season, May showed a strong correlation (R = 0.53) and a minimal PBIAS (3.14%), reflecting a relatively close match with observed rainfall. In contrast, June, July, and August displayed declining correlations (0.49, 0.43, and 0.42, respectively) with increasingly negative PBIAS values (-18.37%, -33.18%, -18.50%), suggesting systematic underestimation. September, the final month of SWM, correlated 0.41 with a low PBIAS (4.28%), indicating a reasonable match.

During the Second Inter-Monsoon (SIM) season, October exhibited a moderate correlation (0.42) with a PBIAS of 9.61%, whereas November showed slightly improved correlation (0.45) but a substantial overestimation (PBIAS = 44.09%).

In the Northeast Monsoon (NEM) season, December displayed a strong correlation (0.71) with an overestimation trend (PBIAS = 22.39%). Similarly, January and February exhibited strong correlations (0.58 and 0.62) with positive biases of 26.49% and 33.88%, respectively, indicating systematic overestimation throughout this season.

The seasonal cumulative precipitation values are shown in Table 2. During the FIM, observed cumulative rainfall was 2426 mm, while NASA Power estimated 3773 mm—an inflation of nearly 55%. This large discrepancy was consistent with the spurious rainfall contributions from dry days, which disproportionately affected seasons with fewer rainfall events.

Table 1 – Monthly R and PBIAS Values for NASA POWER vs. Observed Precipitation

Month	R	PBIAS	Season
1	0.58	26.49%	NEM
2	0.62	33.88%	NEM
3	0.39	45.47%	FIM
4	0.24	61.71%	FIM
5	0.53	3.14%	SWM
6	0.49	-18.37%	SWM
7	0.43	-33.18%	SWM
8	0.42	-18.50%	SWM
9	0.41	4.28%	SWM
10	0.42	9.61%	SIM
11	0.45	44.09%	SIM
12	0.71	22.39%	NEM

A similar pattern was seen in the SIM and NEM, where NASA Power totals exceeded observations by 1303 mm and 1140 mm, respectively, again reflecting the artificial addition of precipitation on days that should have been dry. In contrast, the SWM season, which had the highest rainfall (≈9500 mm observed across 1917 days), was underestimated by NASA (8498 mm). Here, the frequent and intense monsoon rains reduced the relative influence of dry-day overestimation, and the bias was instead driven by NASA's inability to fully capture high-intensity rainfall events. Overall, these seasonal totals confirmed that dry-day overestimation was the primary driver of positive biases in FIM, SIM, and NEM, while underestimation during SWM stemmed from misrepresentation of monsoon-driven rainfall intensity.

Table 2 – Seasonal Total Rainfall Values

Season	Observed Total Rainfall (mm)	NASA Power Total Rainfall (mm)	Count days
FIM	2426.14	3773.14	753
NEM	4404.48	5544.4	1017
SIM	5116.56	6419.66	667
SWM	9533.15	8498.3	1917

3.2 Evaluation of Average Temperature

A comparison of daily temperature values across months revealed a noticeable offset in the NASA POWER temperatures, as shown in Figure 3, which is attributed to a scaling factor. To address this discrepancy, the delta method was applied to each month's data, as detailed in Table 3.

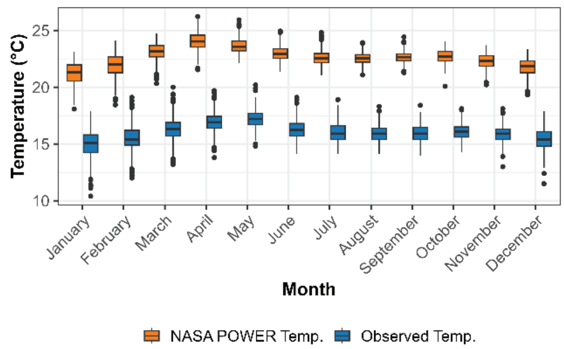

Figure 3 – Boxplot of Daily Observed Temperature vs NASA Power Temperature Data (2009-2021)

Table 3 - Average Temperature Bias Correction

Month	Observed Average Temperature (^{0}C)	NASA Power Average Temperature Data (^{0}C)	Bias (^{0}C)
1	14.91	21.22	-6.31
2	15.51	21.93	-6.42
3	16.32	23.12	-6.80
4	16.95	24.05	-7.10
5	17.21	23.70	-6.50
6	16.33	22.98	-6.65
7	16.01	22.58	-6.58
8	15.92	22.54	-6.62
9	15.95	22.63	-6.69
10	16.04	22.70	-6.66
11	15.88	22.28	-6.40
12	15.41	21.75	-6.34

Figure 4 shows the bias-corrected NASA POWER temperatures compared with the observed temperature data. Overall bias-corrected average temperature data demonstrated a strong correlation coefficient of R = 0.66, with a root mean square error (RMSE) of 0.82. These results indicate a reliability and accuracy in the bias-corrected NASA POWER reanalysis temperature data.

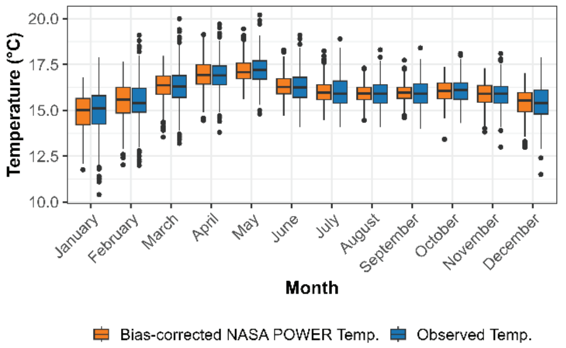

Figure 4 - Boxplot of Daily Observed Temperature vs Bias-Corrected NASA Power Temperature Data (2009-2021)

Further analysis of individual months (Table 4) revealed varying levels of agreement between the bias-corrected NASA POWER and observed temperature data. RMSE values ranged from 0.65 (July) to 1.12 (February), with relatively larger errors in the early months of the year and improved accuracy during the mid-year period. Correlation coefficients (R) varied from 0.31 (October) to 0.62 (July), indicating moderate associations overall. The strongest agreement occurred in the mid-year months of June–August (RMSE ≤ 0.69; R ≥ 0.46), whereas weaker performance was observed in February, March, and October (higher RMSE and lower R values). These results suggest that the bias correction performs best during the mid-year period, while seasonal transitions present greater challenges.

Table 4 - Monthly Statistics for Observed and Bias-Corrected NASA POWER Temperatures

Month	RMSE	R
1	1.07	0.55
2	1.12	0.43
3	1.01	0.39
4	0.88	0.42
5	0.78	0.40
6	0.68	0.61
7	0.65	0.62
8	0.67	0.46
9	0.69	0.45
10	0.77	0.31
11	0.73	0.39
12	0.77	0.61

This finding aligns with a study conducted in Indonesia [11], which also reported temperature discrepancies in weather station data. These results underscore the importance of identifying and correcting such anomalies before utilising NASA POWER data for analysis.

3.3 Evaluation of Average Wind Speed

Comparison of daily wind speed values across months (Figure 5) showed generally good agreement with NASA POWER data, though higher observed wind speeds were underestimated.

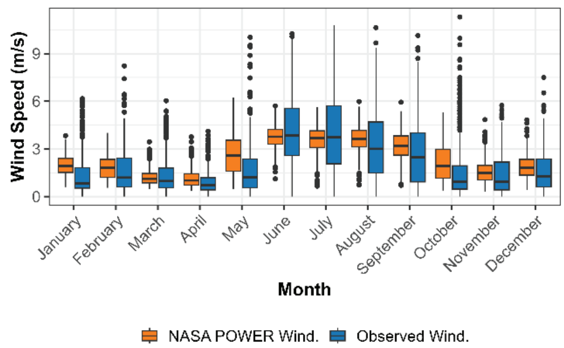

Figure 5 - Boxplot of Daily Observed Wind Speed vs NASA Power Wind Speed Data (2009-2021)

The overall correlation was strong (R = 0.72), with a mean error of 1.12 and an RMSE of 1.46, confirming the reliability of NASA POWER wind speed estimates.

The month-wise analysis presented in Table 5 indicates that ME values range from 0.66 (April) to 1.59 (July), while RMSE values vary between 0.84 (April) and 2.04 (July). The weakest performance is observed in July, with the highest ME (1.59) and RMSE (2.04), indicating a substantial overestimation of wind speeds by the NASA POWER data. In contrast, April demonstrates the most accurate performance, with the lowest ME (0.66), lowest RMSE (0.84), though its correlation with observations is relatively weak (R = 0.26). Stronger correlations are found in the later months, particularly September (R = 0.75) and October (R = 0.73), suggesting improved consistency between observed and NASA POWER wind speeds during this period.

Table 5 - Monthly Statistics for Observed and NASA POWER Wind Speed Data

Month	ME	RMSE	R
1	1.14	1.34	0.39
2	0.95	1.20	0.58
3	0.74	1.03	0.52
4	0.66	0.84	0.26

Table 5 (continued) - Monthly Statistics for Observed and NASA POWER Wind Speed Data

Month	ME	RMSE	R
5	1.27	1.51	0.70
6	1.39	1.80	0.66
7	1.59	2.04	0.68
8	1.46	1.79	0.66
9	1.31	1.60	0.75
10	1.15	1.49	0.73
11	0.90	1.14	0.51
12	0.87	1.08	0.59

3.4 Evaluation of Average Relative Humidity

Comparison of daily relative humidity values across months (Figure 6) showed generally good agreement with NASA POWER data, although periods of low observed humidity were consistently overestimated.

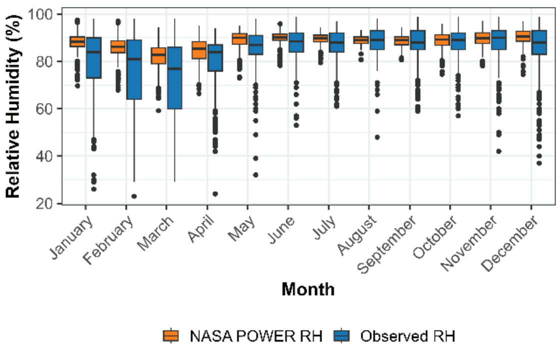

Figure 6 - Boxplot of Daily Observed Relative Humidity vs NASA Power Relative Humidity Data (2009-2021)

The correlation was strong (R = 0.63), but a mean error of 6.52 and an RMSE of 10.40 highlight notable discrepancies.

The month-wise analysis in Table 6 highlighted substantial discrepancies in the first three months of the year. In January, NASA POWER data overestimated relative humidity, with an ME of 9.65 and an RMSE of 14.73, indicating notable bias and variability. February showed even greater deviations (ME = 12.30, RMSE = 17.84), while March remained similarly high (ME = 12.03, RMSE = 16.72), reflecting a systematic overestimation during the early-year period. Correlation coefficients for these months were strong (R = 0.49–0.72), suggesting that while the temporal patterns were partially captured, the magnitudes were consistently higher than observed. From April to December, both ME and RMSE values decreased considerably (ME ≤ 6.67, RMSE ≤ 10.00), indicating improved agreement with observations. Correlation remained variable during the later months (R = 0.33–0.66), with the highest alignment in December (R = 0.66) and lower agreement in August (R = 0.33). Overall, the data revealed a clear seasonal trend: early-year months experienced strong overestimation, whereas mid- to late-year months demonstrated better performance, though some under- or overestimation persisted.

Table 6 - Monthly Statistics for Observed and NASA POWER Relative Humidity Data

Month	ME	RMSE	R
1	9.65	14.73	0.49
2	12.30	17.84	0.65
3	12.03	16.72	0.72
4	6.67	9.99	0.48
5	5.13	7.65	0.47
6	4.68	6.71	0.44
7	4.49	6.24	0.45
8	4.30	5.83	0.33
9	4.55	6.11	0.44
10	4.49	6.57	0.39
11	4.49	7.15	0.53
12	6.07	10.00	0.66

3.5 Evaluation of Average Cloud Cover

A comparison was conducted between observed cloud cover data and NASA POWER reanalysis data for monthly averages from 2017 to 2021. The results showed a strong correlation (R = 0.92), with a mean error (ME) of 0.4 and a root mean square error (RMSE) of 0.5, indicating good agreement between the datasets. These findings further confirm the strong agreement between NASA POWER and monthly observed cloud cover data.

3.6 Long-Term Temperature Trends

The analysis depicted in Figure 7 indicates that the average maximum temperature over the years does not exhibit statistically significant variance, with a p-value of 0.92, a τ value of -0.02, and a Sen's slope of -0.001 °C per year. Conversely, as illustrated in Figure 8, the minimum temperature exhibits an upward trend, with a Sen's slope of 0.01°C per year and a τ value of 0.28, indicating a significant increasing trend with a p-value of 0.03.

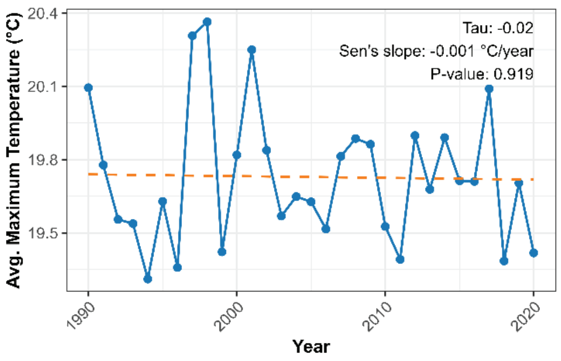

Figure 7 - Average Maximum Temperature Trend analysis

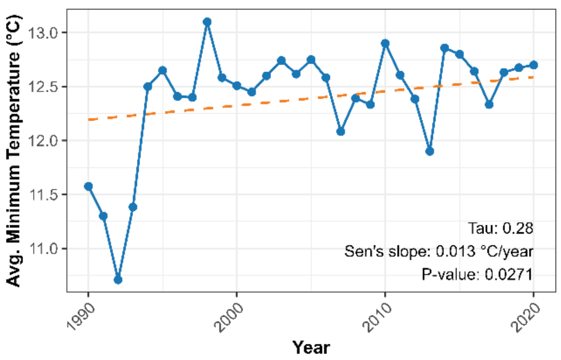

Figure 8 - Average Minimum Temperature Trend analysis

Fluctuations in temperature over time and scales are influenced by a variety of factors, including atmospheric and oceanic conditions, land cover alterations, and localised processes specific to a given area [12]. The study area showed minimum temperature exhibited greater variability compared to the maximum temperature. The findings reveal that nighttime temperatures have experienced a more rapid increase and are more responsive to warming compared to maximum temperatures due to the shallower boundary layer near the ground. During the night, the boundary layer of the atmosphere becomes shallow, which means that a smaller volume of air is involved in heat exchange with the surface. This can lead to stronger changes in nocturnal temperatures because the heat is more concentrated in this smaller volume. As a result, even small perturbations in heat (such as changes in cloud cover, soil moisture, or atmospheric composition) can lead to more significant increases in temperature [13].

3.7 Long-Term Average Wind Speed Trends

The analysis presented in Figure 9 clearly indicates a significant decreasing trend in wind speed over the years, with a p-value of 2.9×10^{-5}, a τ value of -0.53, and a magnitude of -0.029 m/s per year.

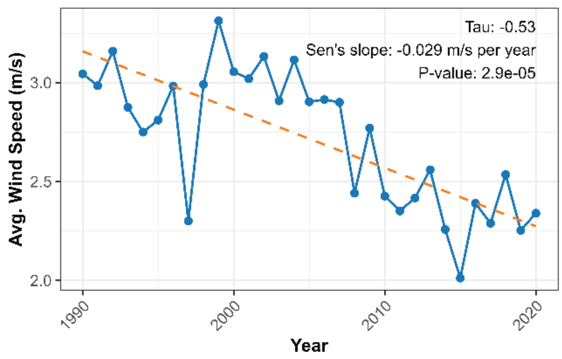

Figure 9 - Average Wind Speed Trend analysis

The decline in wind speed can be influenced by various factors, including global warming, changes in regional and global atmospheric circulation, and human activities such as alterations in land use and air pollution. The temperature difference between land and ocean plays a significant role in wind dynamics [14]. Given the observed increase in minimum temperatures over the past three decades, it is plausible that this land–ocean temperature gradient has weakened, thereby contributing to the reduction in wind speed during the same period. Further research is required to provide a detailed understanding of these complex interactions in this area.

3.8 Long-Term Average Relative Humidity Trends

The data obtained from the Natural Resource Management Centre, Department of Sri Lanka, included mean morning and evening relative humidity values, which were aggregated to monthly relative humidity values. The analysis presented in Figure 10 reveals a discernible increasing trend in the area, with a τ value of 0.31. This upward trend is statistically significant, as indicated by a p-value of 0.015, with a calculated value of 0.19% per year denoting a consistent rise in relative humidity levels annually.

Reduced wind speeds can slow the rate of evaporation from surfaces such as soil, water bodies, and vegetation, thereby adding less moisture to the atmosphere. At the same time, weaker air mixing limits the dispersion of the evaporated moisture, which can lead to localized increases in humidity, as reflected in the data. A more detailed analysis is required to provide further insights and confirm this pattern.

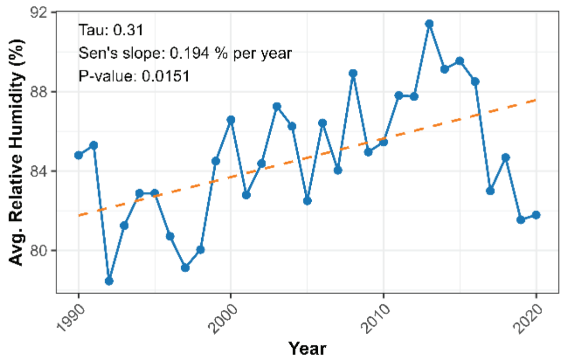

Figure 10 - Average Relative Humidity Trend Analysis

3.9 Long-Term Rainfall Trends

Rainfall data spanning the last 30 years reveals a decreasing trend as shown in Figure 11, with a τ value of -0.13 and Sen's Slope of -7.67 mm per year. However, this observed trend is not statistically significant, as indicated by a p-value of 0.31.

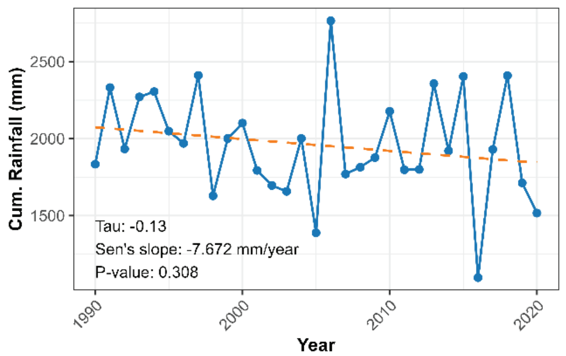

Figure 11 - Cumulative Rainfall Trend analysis

Given the observed reduction in wind speed, it is essential to further investigate the potential implications for the monsoon system, which is largely driven by wind patterns.

3.10 Long-Term Average Short Wave Radiation Trends

NASA Power reanalysis data were utilised to assess trends over the past 30 years due to the absence of observed values for shortwave radiation. The analysis presented in Figure 12 demonstrates an increasing trend, with a τ value of 0.32 and Sen's Slope of 0.2 W/m^2 per year. This trend is statistically significant, with a p-value of 0.013.

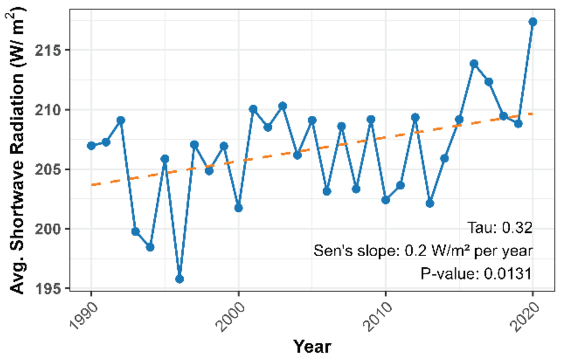

Figure 12 – Average Short Wave Trend analysis

Missing data for some months were supplemented using NASA Power reanalysis data for the Seetha Eliya WS. Monthly data bias-correction (delta method) was applied to temperature data based on available monthly data. For relative humidity and windspeed, missing data were replaced with NASA Power Reanalysis data due to its strong correlation with observed data from the Nuwara Eliya Weather Station. In the case of Rainfall, complete monthly data spanning from 1990 to 2020 were available for analysis. While the use of reanalysis data is a common approach to address data gaps, it may influence the trend analysis by potentially smoothing local variability or underrepresenting extreme events. However, since the substitutions were limited to months with missing records and supported by strong correlations with observed data, their overall effect on the long-term trends is expected to be minimal.

4. Conclusion

This study contributes to evaluating the suitability of NASA POWER reanalysis data for high-elevation, data-scarce regions by using observations from Nuwara Eliya, Sri Lanka. While discrepancies were noted in certain variables, particularly temperature, the results show that the delta method bias-correction can enhance accuracy and usability. The broader analysis of long-term climate trends highlights increasing minimum temperatures and shortwave radiation, alongside declining wind speeds—changes that may significantly affect local agriculture, water resources, and ecosystem dynamics.

These findings underscore the value of reanalysis data as a supplemental resource in regions with limited ground observations. However, the necessity for localised bias correction remains critical to ensuring its reliability in applied climate studies. The outcomes of this study support the integration of corrected NASA POWER reanalysis datasets into climate resilience planning, modelling efforts, and environmental management specifically for the Nuwara Eliya region, and suggest that similar approaches can be adopted in other regions with comparable topographic and data limitations.

Acknowledgement

The authors acknowledge the NASA Langley Research Centre POWER Project, funded by the NASA Earth Science Directorate Applied Science Program, for providing the data. We also thank the Natural Resources Management Centre (NRMC) and the Department of Meteorology, Sri Lanka, for supplying the observational data used in this study.

References

1. Jayawardena, I.M.S.P., Darshika, D.W.T.T., and Herath, H.M.R., "Recent Trends in Climate Extreme Indices over Sri Lanka," Am. J. Clim. Change, Vol. 7, 2018, pp. 586–599.

2. Rodrigues, G.C., and Braga, R.P., "Evaluation of NASA POWER Reanalysis Products to Estimate Daily Weather Variables in a Hot Summer Mediterranean Climate," Agronomy, Vol. 11, 2021, p. 1207.

3. White, J.W., Hoogenboom, G., Stackhouse, P.W., and Hoell, J.M., "Evaluation of NASA Satellite- and Assimilation Model-Derived Long-Term Daily Temperature Data over the Continental US," *Agric. For. Meteorol.*, Vol. 148, 2008, pp. 1574–1584.

4. Bai, J., Chen, X., Dobermann, A., Yang, H., Cassman, K.G., and Zhang, F., "Evaluation of NASA Satellite- and Model-Derived Weather Data for Simulation of Maize Yield Potential in China," *Agron. J.*, Vol. 102, 2010, pp. 9–16.

5. Negm, A., Jabro, J., and Provenzano, G., "Assessing the Suitability of American National Aeronautics and Space Administration (NASA) Agro-Climatology Archive to Predict Daily Meteorological Variables and Reference Evapotranspiration in Sicily, Italy," *Agric. For. Meteorol.*, Vols. 244–245, 2017, pp. 111–121.

6. *Mapa, R.B., Ed., The Soils of Sri Lanka, World Soils Book Series, Springer International Publishing, Cham, 2020, ISBN 978-3-030-44142-5.*

7. Natural Resources Conservation Service, "Missing Temperature and Precipitation Data," https://www.nrcs.usda.gov/programs-initiatives/sswsf-snow-survey-and-water-supply-forecasting-program/wetlands-limate-tables, Visited, 2025/06/01.

8. Deng, P., Zhang, M., Bing, J., Jia, J., and Zhang, D., "Evaluation of the GSMaP_Gauge Products Using Rain Gauge Observations and SWAT Model in the Upper Hanjiang River Basin," Atmospheric Res., Vol. 219, 2019, pp. 153–165.

9. Iizumi, T., Takimoto, T., Masaki, Y., Maruyama, A., Kayaba, N., Takaya, Y., and Masutomi, Y., "A Hybrid Reanalysis-Forecast Meteorological Forcing Data for Advancing Climate Adaptation in Agriculture," Sci. Data, Vol. 11, 2024, p. 849.

10. Haldar, S., Choudhury, M., Choudhury, S., and Samanta, P., "Trend Analysis of Long-Term Meteorological Data of a Growing Metropolitan City in the Era of Global Climate Change," Total Environ. Res. Themes, Vol. 7, 2023.

11. Darman, L.P., Januhariadi, Yudha, M.P., and Aslan, "Assessment of NASA POWER Reanalysis Products as Data Resources Alternative for Weather Monitoring in West Sumbawa, Indonesia," E3S Web Conf., Vol. 485, 2024, p. 06006.

12. Mupangwa, W., Chipindu, L., Ncube, B., Mkuhlani, S., Nhantumbo, N., Masvaya, E., Ngwira, A., Moeletsi, M., Nyagumbo, I., and Liben, F., "Temporal Changes in Minimum and Maximum Temperatures at Selected Locations of Southern Africa," Climate, Vol. 11, 2023, p. 84.

13. Davy, R., and Esau, I., "Differences in the Efficacy of Climate Forcings Explained by Variations in Atmospheric Boundary Layer Depth," Nat. Commun., Vol. 7, 2016, p. 11690.

14. Xu, M., Chang, C.-P., Fu, C., Qi, Y., Robock, A., Robinson, D., Zhang, H.-M., and Xu, C., "Steady Decline of East Asian Monsoon Winds, 1969–2000: Evidence from Direct Ground Measurements of Wind Speed," J. Geophys. Res., Vol. 111, 2006.